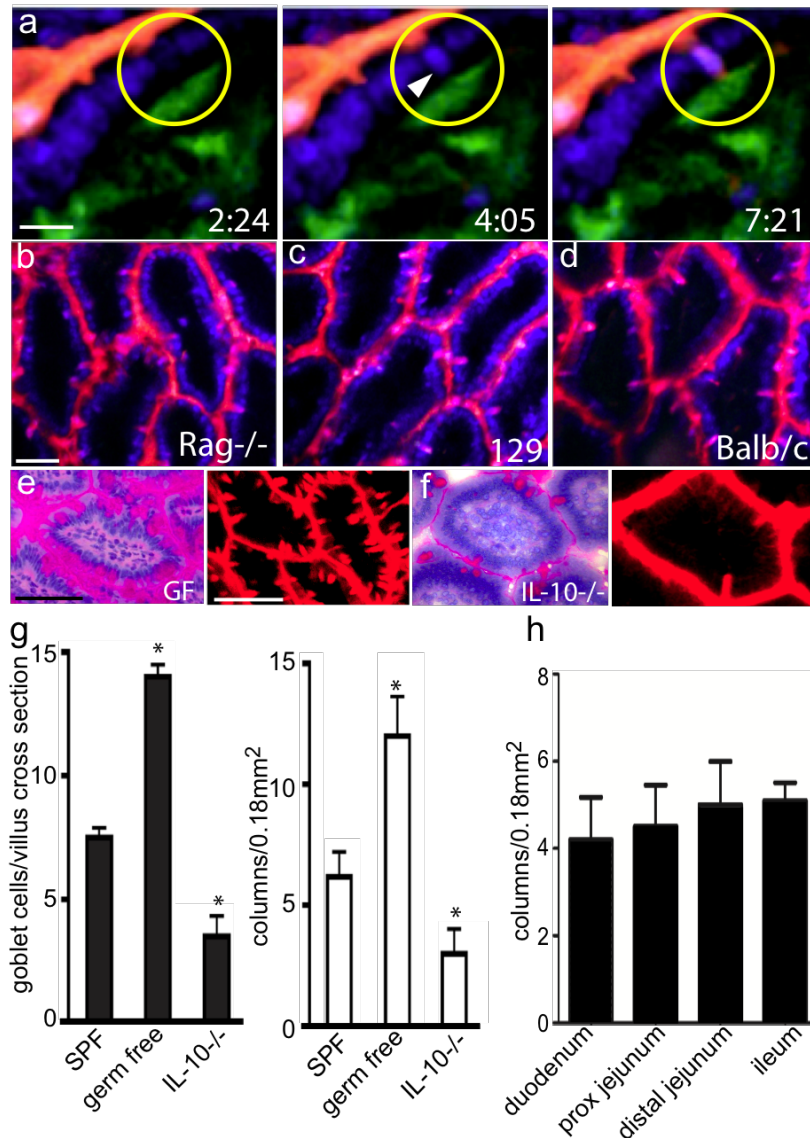
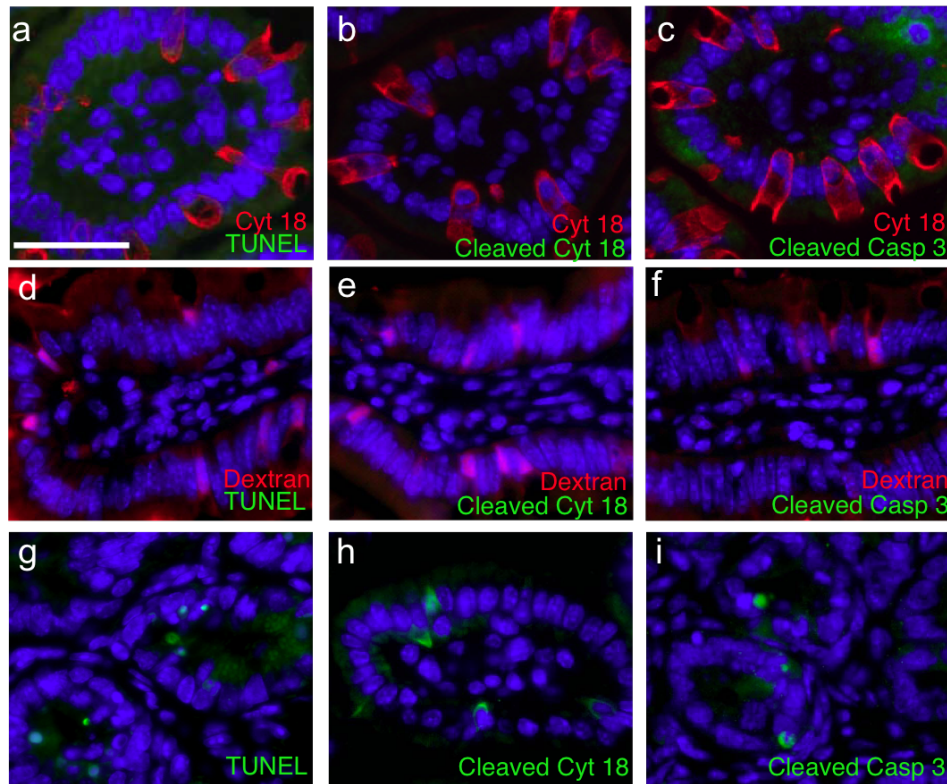


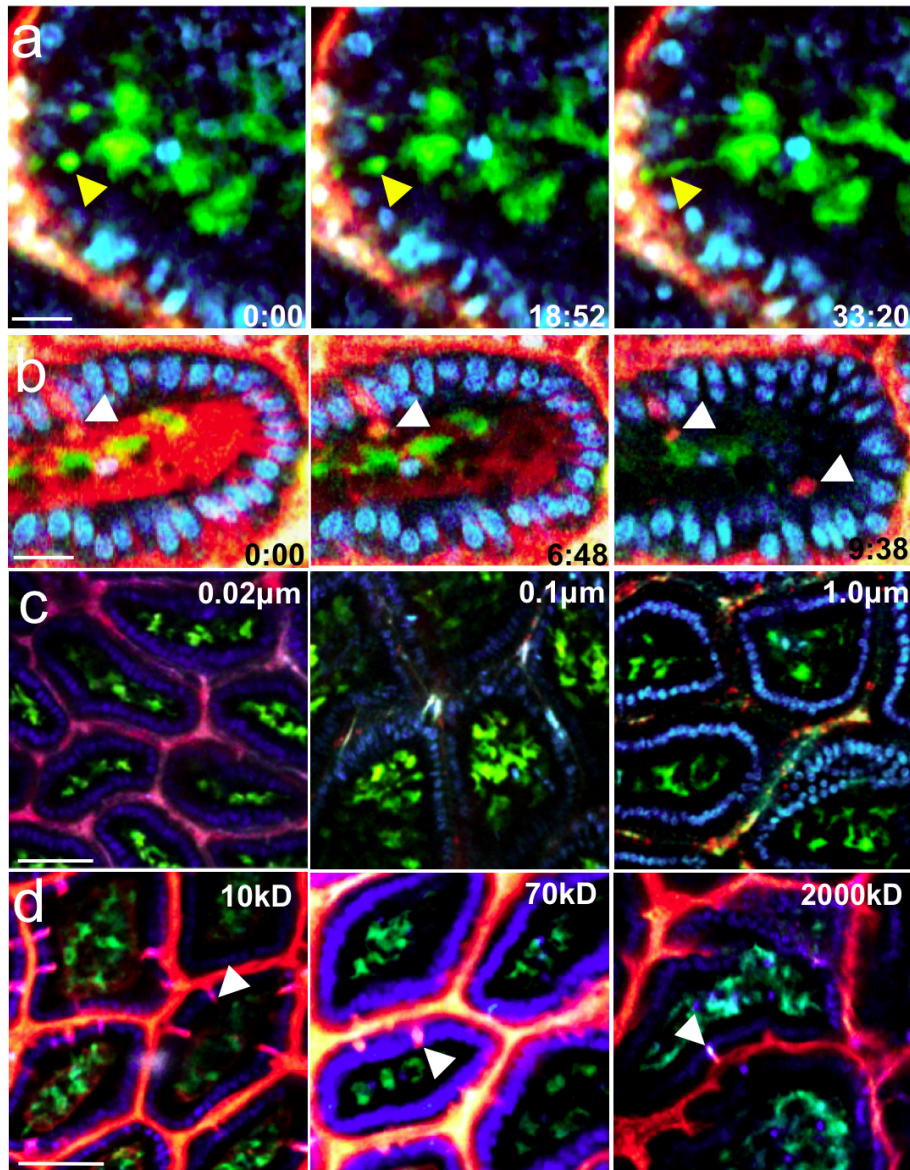
Supplementary Figure 1. Intravital 2P imaging approach and epithelial continuity in the gut. (a) Schematic drawing of the Intravital 2P microscopy preparation and chamber used for gut imaging. A 2 cm sagittal incision is made in the abdominal wall and the intestine is attached to the bottom of the imaging chamber (cover glass) with Vetbond (3M). The imaging chamber is positioned over the animal to seal off the peritoneal cavity and imaging performed with a 0.95 NA 20x Olympus water dipping objective. Imaging can be performed from either the serosal surface or from the luminal surface after making a small incision in the intestine (see exploded view). (b) 3D 2P image acquired from the serosal surface of the small intestine given intra-luminal 10 kD TRITC-dextran (red) showing a column of dextran projecting across the epithelium and terminating near CD11cYFP+ LP-DCs (green). Similar dextran projections were not found in the (c) stomach, (d) cecum, or (e) colon, despite the fact that dextran was clearly visible in the lumen (red); yellow arrows denote dextran filling the (c) gastric glands and (d and e) colonic crypts. Scale bar = 50 μ m.



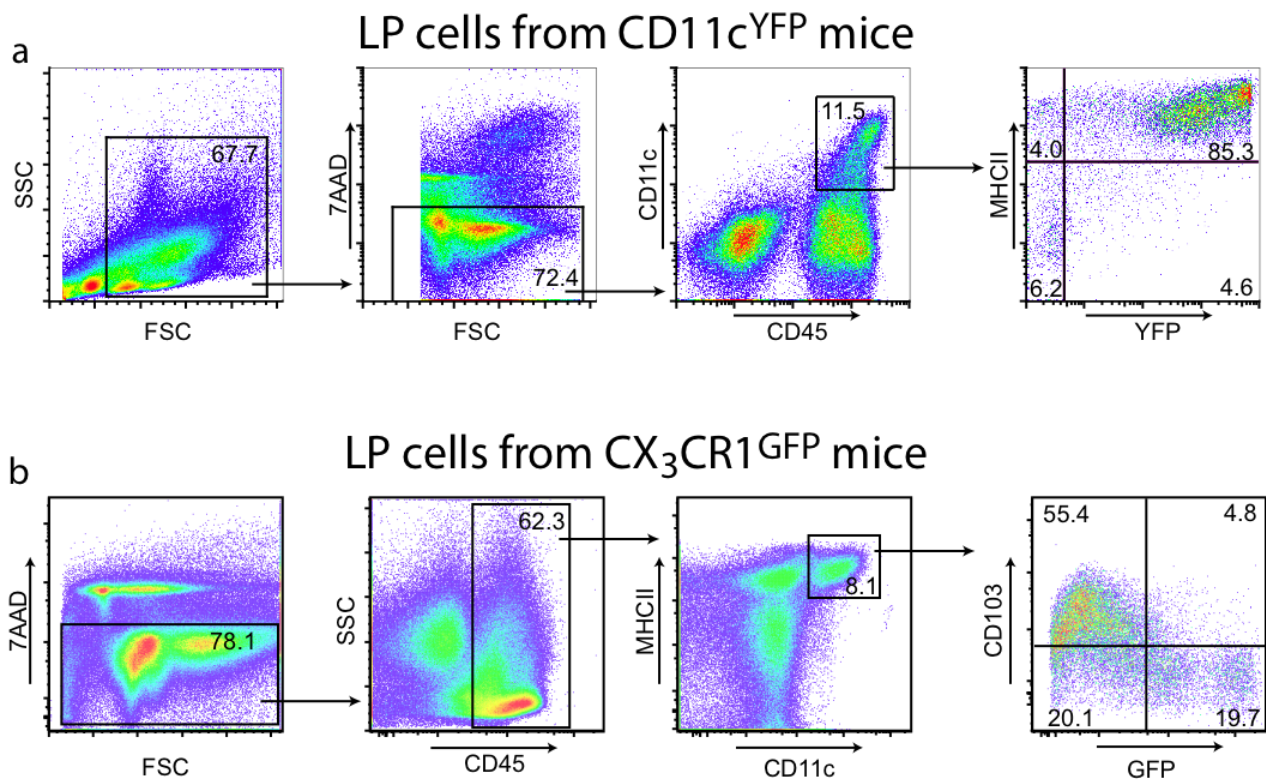
Supplementary Figure 2. Trans-epithelial dextran columns are a common feature throughout the small intestine in multiple mouse strains and correlate with changes in GC numbers. (a) Time lapse 2P images of a trans-epithelial dextran column filling. A DAPI stained nucleus (blue, white arrow) appears shortly before the dextran structure (red) projects across the epithelium toward a LP-DC (green). (b-d) 2P imaging of various mouse strains following the injection of luminal fluorescent dextran revealed that dextran columns (red) extended through the epithelium (DAPI stained nuclei, blue) in (b) Rag^{-/-} mice, (c) 129 mice and (d) Balb/c mice. (e and f) PAS staining (pink, left panels) and 2P imaging of dextran (red, right panels) of small intestine in (e) germ free and (f) IL-10^{-/-} mice revealed a correlation between the presence of GC and trans-epithelial dextran columns. (g) The frequency of GCs and trans-epithelial dextran columns was correlated and significantly increased in germ-free mice ($p = 0.0013$ for PAS, $p = 0.009$ for 2P) and decreased in IL-10^{-/-} mice ($p = 0.017$ for PAS, $p = 0.021$ for 2P) when compared with SPF housed mice. (h) Trans-epithelial dextran columns were present throughout the length of the small intestine with a non-significant trend towards more in the ileum. Scale bar = 30 μ m (a) 50 μ m (b) and 100 μ m (e). Time stamp = min:sec from start of recording.



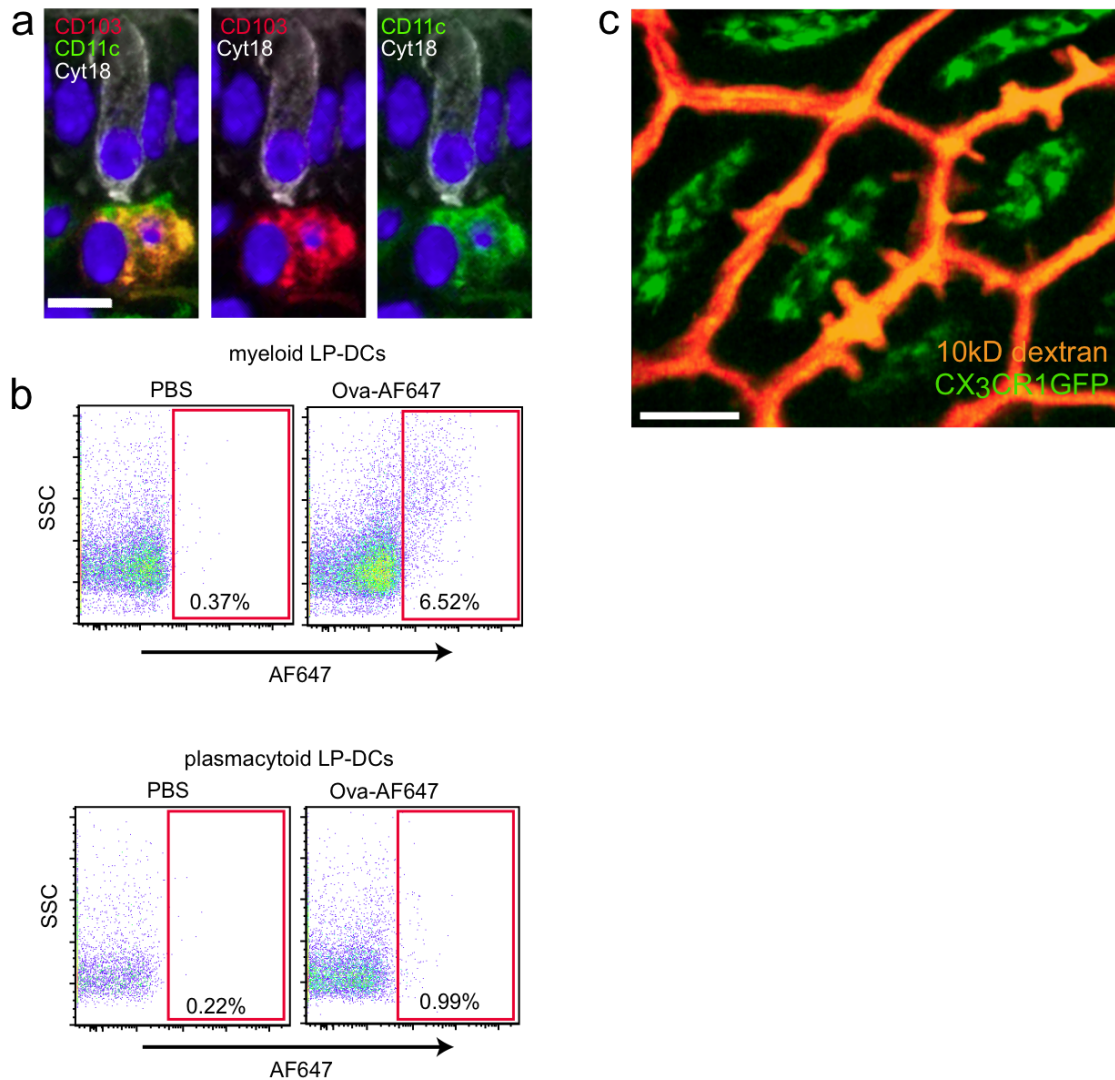
Supplementary Figure 3: GC associated antigen passages (GAPs) are not associated with GC apoptosis. (a-c) Intestines from C57BL/6 mice were evaluated for the presence of apoptosis markers in cytokeratin 18+ GCs. Evaluation of more than eight hundred GCs revealed that 0.23% were TUNEL positive, 0.12% were positive for activated caspase 3, and none were positive for cleaved cytokeratin 18. (d-f) Sixty-five dextran columns from multiple sections and mice given luminal dextran were evaluated for markers of apoptosis and none were positive for the apoptotic markers TUNEL, cleaved cytokeratin 18, or cleaved caspase 3. (g-i) Mice exposed to sublethal irradiation demonstrated positive staining for the above apoptotic markers. Blue = DAPI nuclear stain. Scale bar = 25mm.



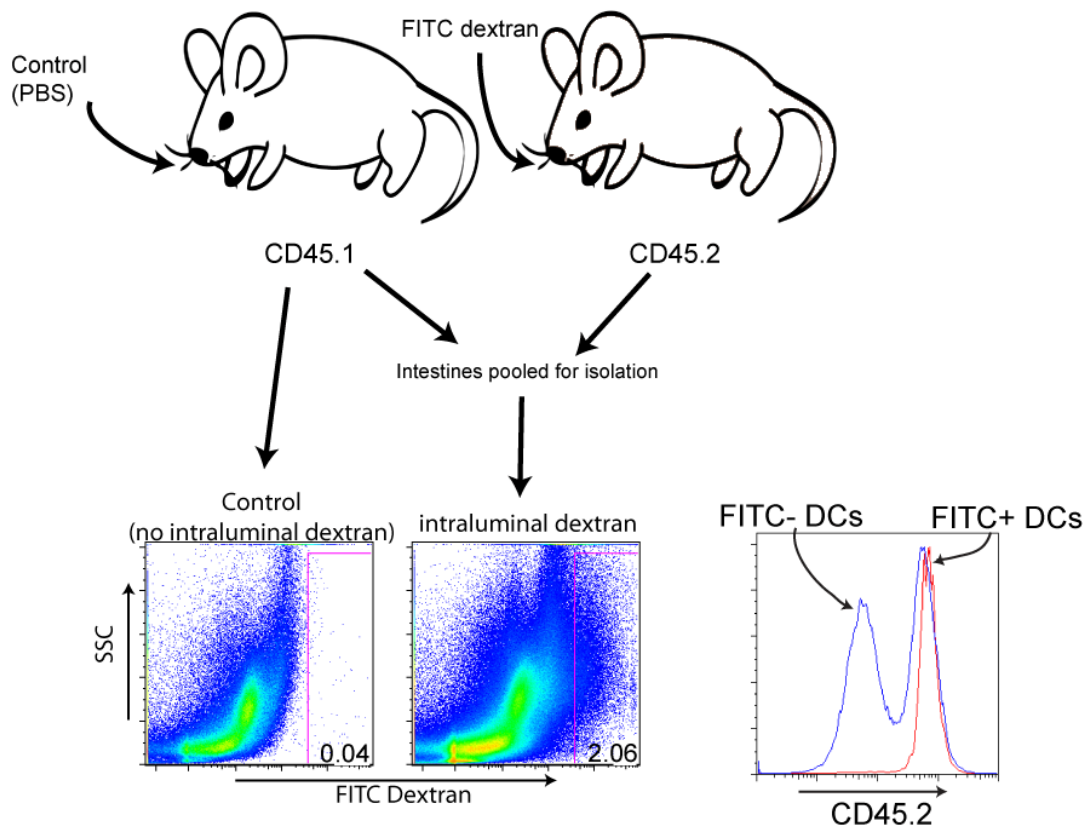
Supplementary Figure 4. GAPs are a main pathway delivering small soluble luminal antigen. 2P imaging of CD11cYFP mice was performed following the intraluminal injection of the model antigens dextran and fluorescent beads. (a) While LP-DCs (green) extended TEDs (yellow arrowheads) in ~2% of villi following infection with *Salmonella*, they did not co-localize with luminal dextran (red). (b) With higher concentrations, 10kD dextran (red) is visible crossing the epithelium (DAPI stained nuclei, blue) by paracellular leak. However, dextran only co-localized with LP-DCs (green) that were closely associated with GAPs (white arrowheads; the lower white arrowhead indicates a GAP protruding into the top of the imaging volume). (c) Fluorescent beads, as small as 0.02 μ m, did not label GAPs. (d) In contrast, GAPs filled with dextrans up to 2000kD (white arrowheads), but were most efficient at delivering antigens <70Kd to LP-DCs. Scale bar = 15 μ m (a and b) and 50 μ m (c and d).



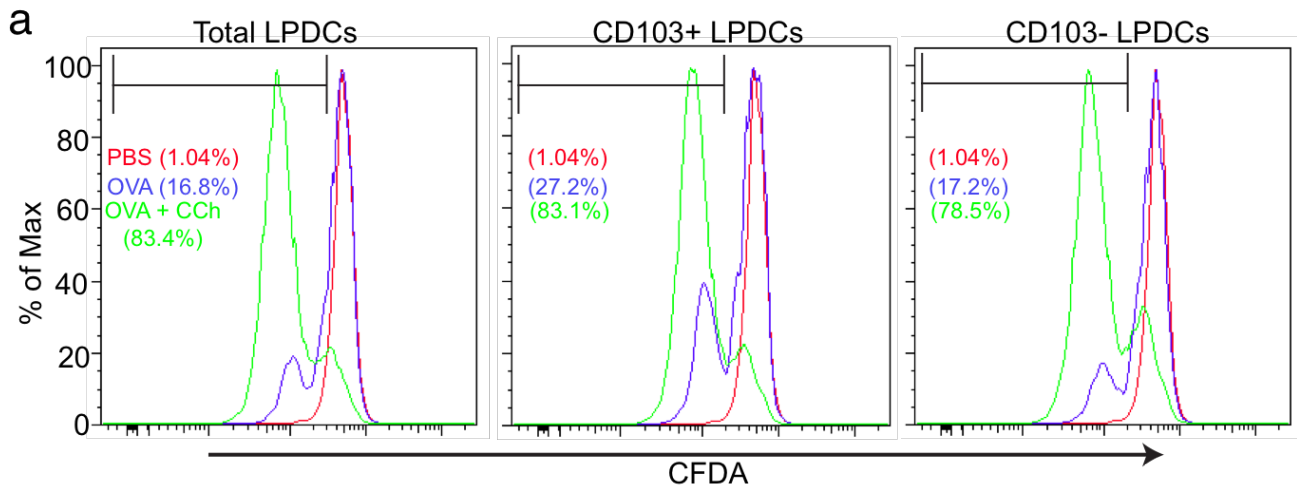
Supplementary Figure 5: Characterization of LP-DC populations in CD11c^{YFP} and CX₃CR1^{GFP} reporter mice. (a) Flow cytometric analysis of LP cells isolated from CD11c^{YFP} reporter mice revealed that YFP expression identified >95% of the LP-DC population. (b) Flow cytometric analysis of LP cells isolated from CX₃CR1^{GFP} reporter mice revealed that > 90% of CD103⁺ LP-DCs were GFP⁻.



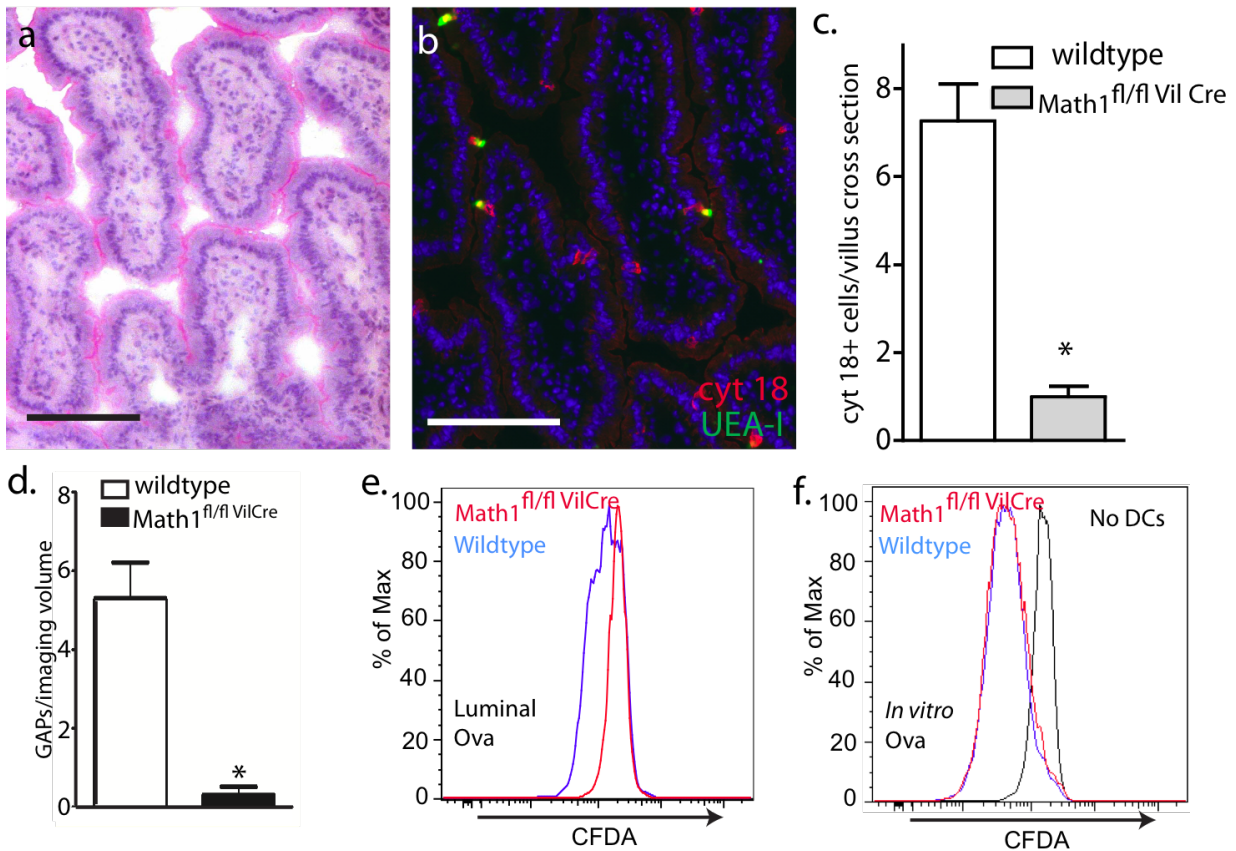
Supplementary Figure 6: CD103+ LP-DCs preferentially interact with GCs in the steady state. (a) CD103+ (red) CD11c+ (green) LP-DCs could be seen interacting with GCs (white, cytokeratin 18+) by immunofluorescence analysis of 5 μ m frozen intestinal sections. Nuclei are stained with DAPI (blue). B220+ CD11c+ plasmacytoid DCs were not seen associating with GCs (data not shown). (b) Flow cytometric analysis of LP-DCs from mice receiving intra-luminal fluorescent Ova-647 revealed that luminal antigen was taken up readily by myeloid (CD45+ MHCII+ CD11c+ CD11b+ PDCA-1-) LP-DCs and only rarely associated with plasmacytoid (CD45+ B220+ PDCA-1+ MHCIIIo) LP-DCs. (c) Analysis of CX3CR1GFP single reporter mice over the course of multiple experiments revealed that CX3CR1GFP+ cells (green) are rarely associated with GAPs (dextran, red) in the steady state. Scale bar = 6.25 μ m (a), 40 μ m (c).



Supplementary Figure 7. LP-DC acquisition of luminal antigen is not a result of antigen release or exchange during cell isolation. PBS or FITC dextran was injected into the lumen of congenic mice expressing the CD45.1 or CD45.2 alleles respectively. Cellular populations were isolated from the intestines of mice given PBS alone or in combination with those from mice given FITC dextran. Flow cytometry on the isolated cellular populations revealed that the FITC+ DCs were CD45.2+, confirming that luminal antigen is not exchanged between DCs during isolation.



Supplemental Figure 8: LP-DCs from mice given carbamylcholine (CCh) have an increased capacity to induce T cell proliferation to luminal antigen. (a) LP-DCs from mice given luminal PBS or luminal Ova and injected subcutaneously with CCh or PBS were assessed for antigen presentation capacity by co-culture with CFDA-labeled OTI T cells. LP-DCs from CCh injected mice given luminal Ova (green histograms) showed enhanced luminal antigen presentation when compared with mice injected with PBS and given luminal Ova (blue histograms). Numbers represent the percentage of cells from each group falling in the divided population gate as determined by the luminal PBS control group (red histograms).



Supplemental Figure 9: *Math1^{fl/fl} Vil Cre* mice lack goblet cells and GAPS, but do not have an inherent defect in antigen presentation by LP-DCs. (a) Periodic Acid Schiff and (b) cytokeratin 18 and UEA-I staining of small intestine sections from *Math1^{fl/fl} Vil Cre* mice revealed a significantly decreased goblet cell population when compared with wildtype controls (c). (d) By 2P analysis GAPS were significantly reduced in *Math1^{fl/fl} Vil Cre* mice when compared with wildtype controls. (e) Antigen presentation assays revealed that CD103⁺ LP-DCs from *Math1^{fl/fl} Vil Cre* failed to stimulate OT-I T cell proliferation following luminal Ova administration as determined by CFDA dilution. (f) LP-DCs from wildtype mice and *Math1^{fl/fl} Vil Cre* mice had equivalent antigen presentation capacity as indicated by CFDA dilution when cultured in the presence of exogenously added Ova (10µg). Scale bars in a and b = 100µm. * = p < 0.05.

Supplementary Movie 1. 2P imaging from serosal or luminal surfaces, 3D reconstruction of dextran projection, and DC probing behavior *in vivo*. CD11c-YFP reporter mice were given luminal dextran (red) and imaged (upper left panel) through the serosal surface into the villi or (upper right panel) from the luminal surface into the villi of the small intestine. (lower left panel) Shows CD11cYFP+ LP-DCs (green) probing the epithelium (DAPI stained nuclei, blue) with dendrites, but not extending dendrites into the lumen (dextran, red). (lower right panel) Shows a 3D reconstruction of a trans-epithelial 10kD dextran column within the villi.

Supplementary Movie 2. Trans-epithelial dextran columns overlying cecal patches. 2P imaging was performed on CD11c-YFP (green) LysM-GFP (blue) dual reporter mice given luminal 10kD dextran (red). Imaging of cecal patches revealed the presence of rare trans-epithelial dextran columns (white arrow).

Supplementary Movie 3. Trans-epithelial dextran columns are associated with epithelial nuclei and are dynamic. 2P imaging was performed on CD11c-YFP reporter mice given luminal 10kD dextran. The movie shows a DAPI stained nucleus (blue) appear minutes before a GAP fills with dextran (red) near a CD11c-YFP LP-DC (green).

Supplementary Movie 4. LP-DCs interact with trans-epithelial dextran columns. *In vivo* 2P imaging was performed on CD11c-YFP reporter mice given luminal dextran. (Left panel) LP-DCs (green) make dynamic interactions with dextran columns (red) that traverse the epithelium (DAPI nuclei, blue). (Right panel) 3D rendered confocal image of a CD11c-YFP+ LP-DC (green) contacting a dextran filled epithelial cell (red) with the nucleus clearly visible (white arrow indicates contact).

Supplementary Movie 5. GAPs are a major mechanism by which LP-DCs acquire luminal antigen *in vivo*. (upper left panel). Rare LP-DC TEDs (green; TED indicated by white arrow) were observed during *Salmonella* infection, but did not co-localize with luminal dextran (red). (upper right panel) At higher concentrations, 10kD dextran flooded across the epithelium (DAPI stained nuclei, blue) into the LP via paracellular leak, but was flushed from the LP and did not co-localize with LP-DCs, with the exception of dextran delivered via GAPs (white circle). GAPs delivered various model antigens (lower left panel) 10kD dextran (red) and (lower right panel) BSA (red) to LP-DCs (green) across the epithelium (DAPI nuclei, blue).

Supplementary Movie 6. GAPs deliver luminal OVA to LP-DCs. *In vivo* 2P imaging was performed on CD11c-YFP reporter mice given luminal fluorescent Ova 647. Ova (red) is delivered across the epithelium (DAPI nuclei, blue) via GAPs to LP-DCs (green).